GL 01608

MAGNETOTELLURIC OBSERVATIONS AT THE ROOSEVELT HOT SPRINGS KGRA AND MINERAL MTS, UTAH

Philip E. Wannamaker, William R. Sill, and Stanley H. Ward

Dept. of Geology and Geophysics, University of Utah

Twenty-five magnetotelluric soundings in the Roosevelt Hot Springs area indicate a very complicated, three-dimensional electrical environment. The assembly of a profile of one-dimensional transverse electric inversion interpretations yields a calculated 2-D apparent resistivity-frequency pseudosection far removed from the observed data. Trial-and-error modeling improves the fit only a little. The most notable difficulty, the presence in both TE and TM pseudosections of pronounced contrasts in ρ_a persisting to the lowest observed frequency, may be explained by the discontinuities in electric field that are found for all directions of wave excitation for 3-D geometries.

The estimation of electrical strike is also difficult in the 3-D case since the total fields do not decompose into the two principal excitation modes. Whenever a plane of symmetry exists, the estimated electrical strike will be normal to it; otherwise an oblique estimation results. The observed consistency of strike estimation at Roosevelt is likely due to the gross, elongate, resistive horst structure of the Mineral Mts. in surrounding conductive valley fill.

Mode identification and the effects of near-surface 3D inhomogeneities pose potential major limitations to the magnetotelluric method.

ROOSEVELT HOT SPRINGS KGRA
LOCATION OF MT SOUNDINGS   FIG. 1.

Previous active source electrical and electromagnetic measurements show a range of interpreted true resistivities spanning 3 to 10^3 *-m at the Roosevelt Hot Springs KGRA. Contour pattern lows of first separation dipole-dipole apparent resistivity values are roughly coincident with highs of near-surface thermal gradient measurements. During the summer of 1976, twenty-five magnetotelluric (MT) soundings were obtained in the vicinity of the Roosevelt Hot Springs in an attempt to describe any possible deep convective heat source for the conductive hydrothermal system (see Figure 1).

Sources of electrical conductivity to consider are electrolytic conduction through pore passages, surface conduction along mineral surfaces, thermally activated semiconduction, and electrolytic conduction in wet, partial melts. The Basin and Range tectonic province conductivity model of W. F. Brace in the AGU Monograph 14 (1971) is used as a rough standard by which to judge the observed MT results. Petrological work on the Mineral Mts. rhyolitic volcanics indicated substantial magma chambers existed at depths of 1.6 to 12 kms as little as 0.5 m.y. ago. Any present-day partially molten magmas may be detected electrically.
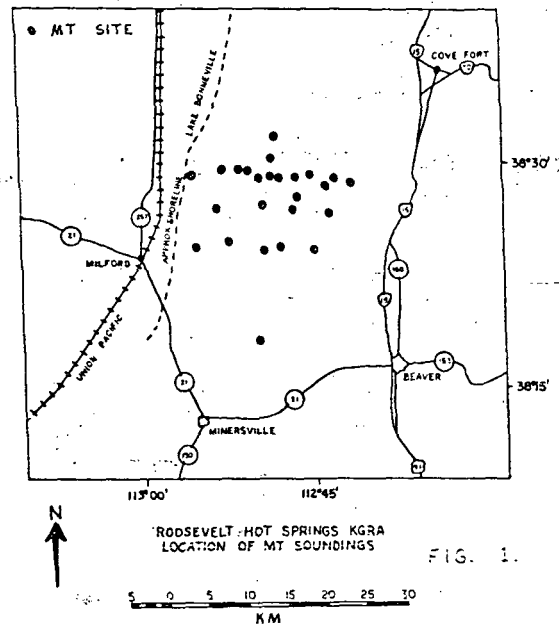
As is the standard procedure, 1-D layered and continuous inversions of the transverse electric (TE) data for several individual sites were performed. In the conductive Milford Valley graben, values of apparent resistivity drop to 0.10 Ω-m for the lowest frequencies of observation and interpreted true resistivities are low by a factor of 5 to 10 while interface depths are too shallow by a factor of 2 or more.

Multifrequency apparent resistivity data for a profile of 12 MT stations is presented in the form of frequency-distance pseudosections for both TE and TM modes of wave excitation (see Figs. 2 and 3). The major difference between the two pseudosections involves the overall level of ρ_a values. Except perhaps for the westernmost stations on conductive valley fill, the TM values generally exceed those of TE by a factor of about ten. One important common characteristic is the presence of pronounced, station-to-station apparent resistivity contrasts enduring to the lowest frequency of observation at two of the sites. For use as an interpretational starting point, the best-fit discrete-layer inversion results for each of the twelve stations in the profile were stitched together to form a crude,
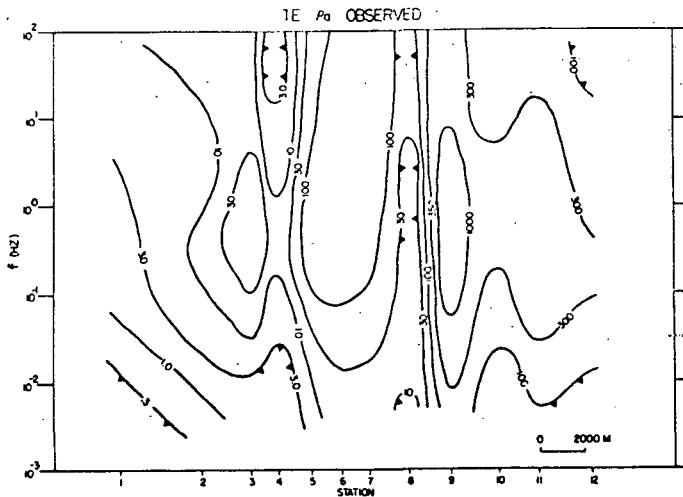
TE ρa OBSERVED

Fig. 2: Observed TE apparent resistivity pseudosection for 12-station profile. Contours in Ω-m.
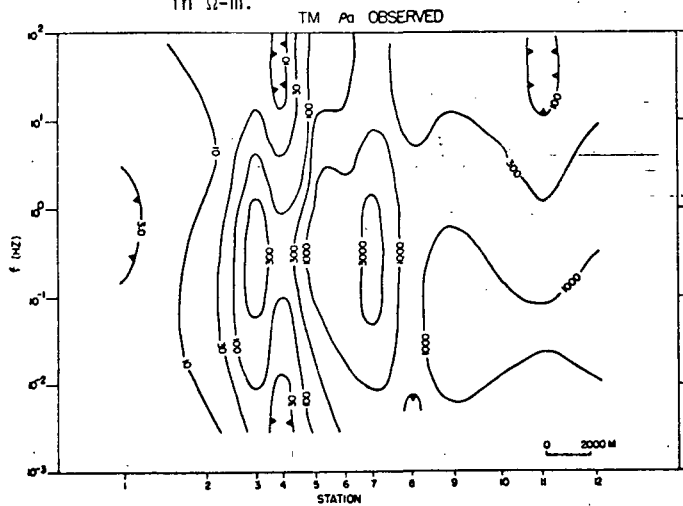
TM ρa OBSERVED

Fig. 3: Observed TM apparent resistivity pseudosection for 12-station profile. Contours in Ω-m.

initial 2-D estimate of the resistivity structure (see Fig. 4). The computed TE, 2-D pseudosection for this ensemble matches the observed ρ_a section only for the stations in the conductive graben and for the very high frequency values for the rest of the stations (Fig. 5). Trial-and-error attempts at improving the basic model yield an adequate fit only down to about 0.5 Hz whereafter the degeneration of agreement is marked (see Figs. 6 and 7). A TM pseudosection calculation for the 1-D assembly agrees very well with the observed TE contours however TE modelled does not agree whatsoever with TM observed so a mere mode misidentification is not the answer (Fig. 8).
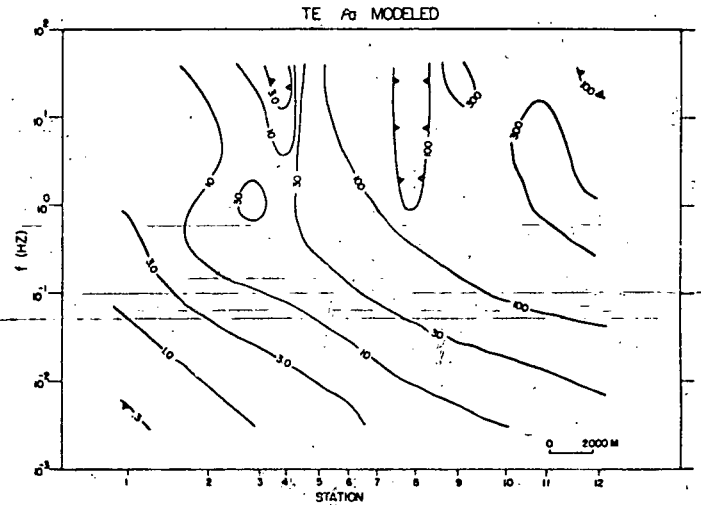
TE ρa MODELED

Fig. 5: Computed, 2-D, TE pseudosection for 1-D stitch model. Contours in Ω-m.

1-D INVERSIONS ASSEMBLED INTO CRUDE 2-D MODEL

0   2 KM

Fig. 4: Discrete-layer, 1-D inversion stitch model for 12-station profile. Values in Ω-m.

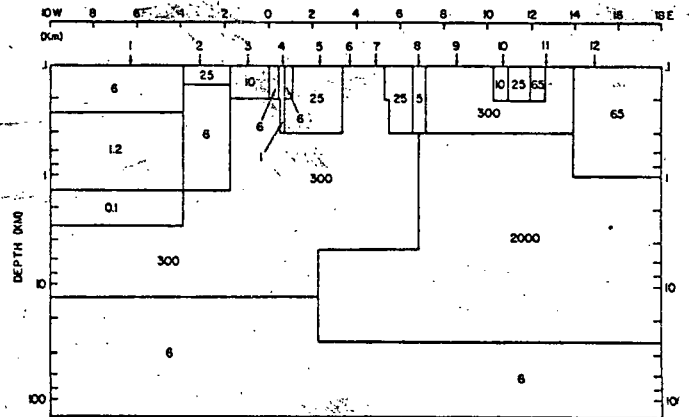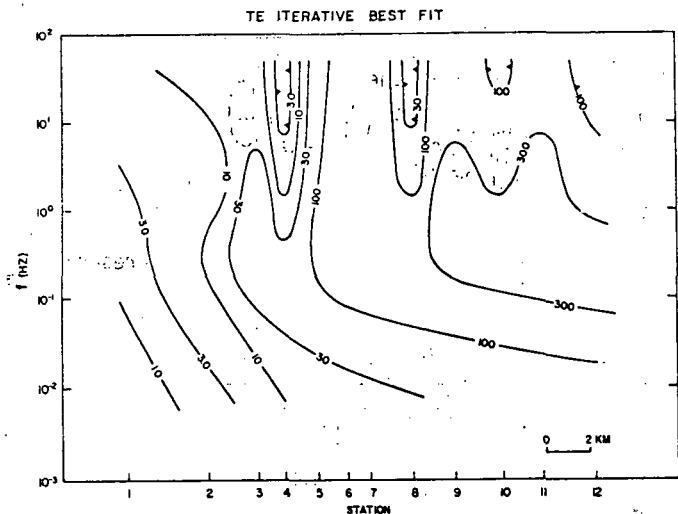**Fig. 7:** Best-fit TE resistivity model for 12-station profile. Values in Ω-m.

Fig. 6: Trial-and-error best-fit 2-D TE pseudo-
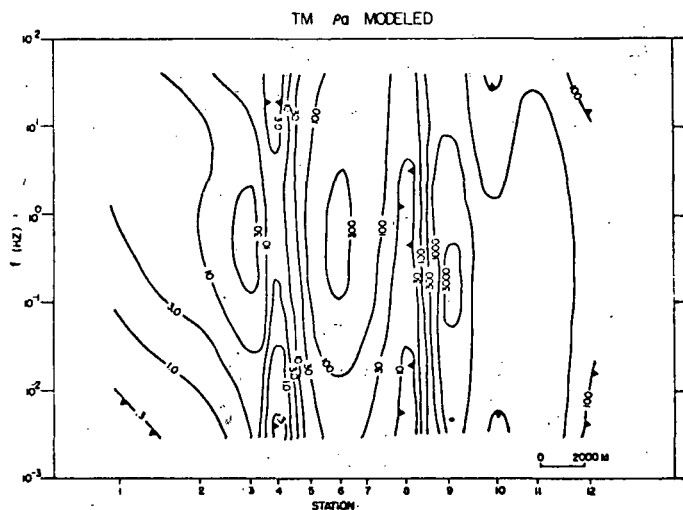section for 12-station profile. Contours
in Ω-m.

Fig. 8: Computed, 2-D, TM pseudosection for 1-D
stitch model. Contours in Ω-m.

$W = 280$ m
$d = 280$ m
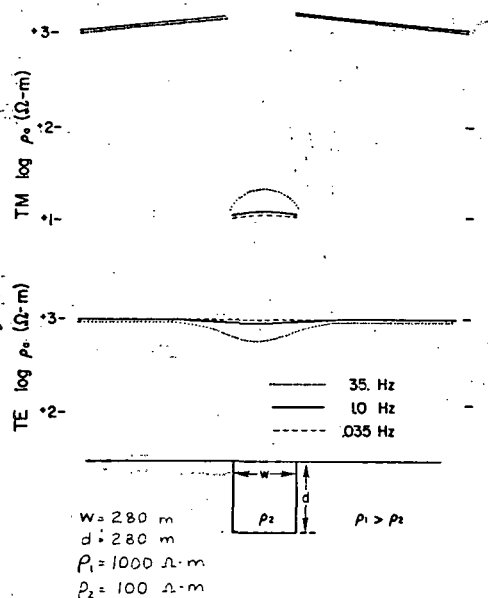$\rho_1 = 1000$ Ω·m
$\rho_2 = 100$ Ω·m

Fig. 9: TM and TE multifrequency profiles for
single, outcropping, shallow, 2-D
conductor.
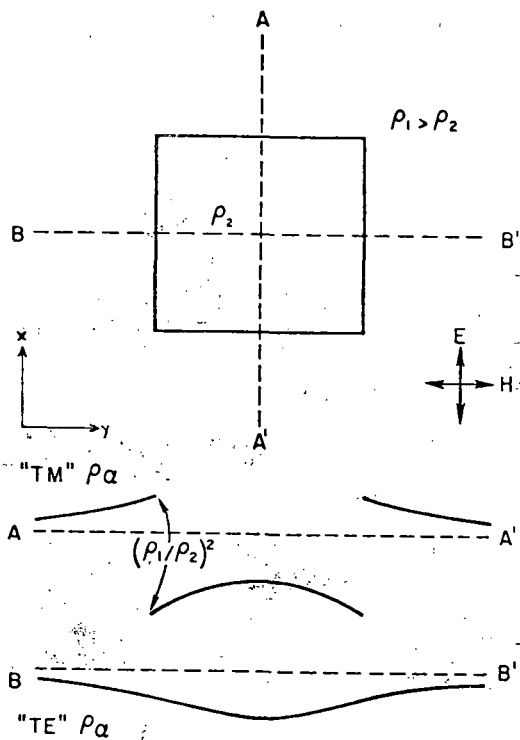
Fig. 10: Conductive rectangular prism in resistive
environment plus proposed apparent resis-
tivity signatures for single polarization
of electric vector.

Some outcropping, single conductor, multi-
frequency, TE and TM model results may explain
some of the problems in terms of 3-D effects
(Fig. 9). In the 2-D, TE model, continuity of
tangential electric field (E_t) parallel to media
boundaries requires a continuous apparent resis-
tivity function for all frequencies. In the TM
model, the electric vector is orthogonal to the
media contacts, normal current density (J_n)
must be continuous, and so the total electric
vector at the contacts will be discontinuous by
a factor of (ρ_1/ρ_2). For the TM case, $\rho_a \sim E^2$ so
one expects and observes a (ρ_1/ρ_2)^2 disconti-
nuity at vertical contacts for all frequencies.
Please note that the apparent resistivity
values within the prism are greatly depressed
below the true value while those outside are
only slightly elevated w.r.t. the true resis-
tivity. The anomaly for a simple, outcropping,
conductive 3-D prism will possess

characteristics of both TE and TM 2-D models (see Fig. 10). Measurements along line A-A' (with E normal to the resistivity discontinuity) will yield a profile resembling a TM excitation. Continuity of J_n requires that the $(\rho_1/\rho_2)^2$ discontinuity in ρ_a be present for all frequencies. Measurements along line B-B' (with E parallel to the resistivity discontinuity) will give a profile resembling a TE situation. Continuity of E_t requires a smooth ρ_a curve. Analogous $\rho_a(\omega)$ profiles will appear for an E polarization orthogonal to that depicted. Line A-A' would be "TE" and line B-B' would be "TM". Hence, finally, a map view of the anomaly of this 3-D body will consist of pronounced ρ_a contours lasting down to the lowest frequency measured. Since in the field both E_x and E_y are present, then regardless of which observed pseudosection (TE or TM) is chosen, a profile across a conductive prism of finite strike length will exhibit such exaggerated, persisting contrasts in ρ_a. The enclosed pseudosections contain examples of this very phenomenon and they cannot be fit by any purely two-dimensional model.

Depth of exploration is another problem in 3-D environments. A 2-D, TM model of a deeply extending conductive model is very similar to the previous shallow model and one may reason as above that the 3-D anomalies will also be very similar. MT soundings within such 3-D conductive prisms may provide no meaningful information about deeper structures.

The plane wave mode identification (ie. estimation of electrical strike) is also difficult in the 3-D case. Standard strike estimation procedures assume approximate two-dimensionality where the vertical component of magnetic field, Hz, is linearly related to, or completely coherent with only the component of E parallel to strike (say E_x). The relation is defined by Maxwell's second equation, in the general case, as

$$H_z = \frac{-1}{i\omega\mu_o}\left[\frac{\partial E_x}{\partial y} - \frac{\partial E_y}{\partial x}\right]$$

In the 2-D case, $\partial/\partial x = 0$ so the above reduces to

$$H_z = \frac{-1}{i\omega\mu_o}\frac{\partial E_x}{\partial y} = Y_{zx}E_x$$

where Y_{zx} is the admittance. In the field, neither measurement electrode is likely to be parallel to strike and a component of E_x will be in each electric record. If x' and y' represent the measurement axes, then one must write

$$H_z = Y_{zx'}E_{x'} + Y_{zx'}E_{y'}$$

where $Y_{zx'}$ and $Y_{zy'}$ are the relevant admittance functions determined by standard spectral analysis techniques. The patent approach is to rotate mathematically the measurement axes to maximize $Y_{zx'}$ and the corresponding x'-direction is estimated strike. In three dimensions, however, Hz no longer depends on a single direction of electric vector. Referring to Fig. 9, from symmetry observe that along A-A', $\partial/\partial y = 0$, Hz will be wholly related to E_x and the estimated strike will be along the y-axis. Along B-B', $\partial/\partial x = 0$, Hz will be wholly related to E_x and the estimated strike will be along the x-axis. Along diagonals of the prism, both derivatives are important and an oblique estimation will result.

The mode identification for the Roosevelt Hot Springs stations is pretty consistent, however, and parallels the long axis of the Mineral Mts. Regional structure is likely responsible. The mountains form a very elongate, north-south trending resistive body flanked on the west by deep, very conductive alluvium and to a minor extent on the east by the same. Especially for east-west profiles across the central portions of this range, $\partial/\partial y \gg \partial/\partial x$ where x is the north-south axis of the mountains. The consistency in the electrical strike estimation does not appear related to smaller-scale hot-spring structures but instead to the gross topography of the region.
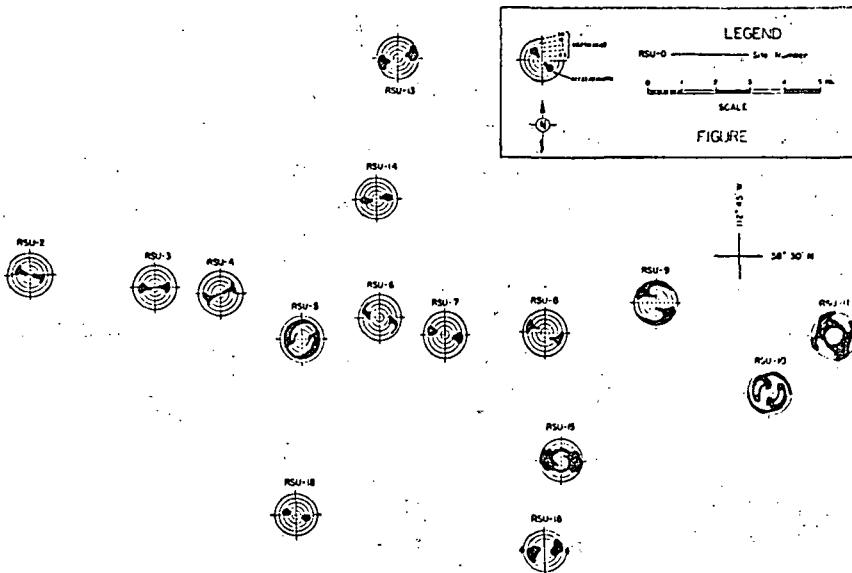

Fig. 11: Dip-axis estimates (A(YZ) is contractor's notation) as a function of depth for several stations in Roosevelt area. Dip-axis is normal to estimated strike and blackened area indicates scatter in calculated axes. Depth is a product of continuous inversion algorithm which provides approximate depth-frequency correspondence listing.